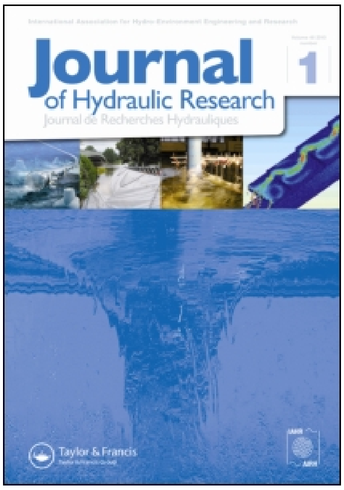

Journal of Hydraulic Research
Publication details, including instructions for authors and subscription information:
http://www.informaworld.com/smpp/title~content=t916282780

A two-layer approach for depth-limited open-channel flows with submerged vegetation

Wonjun Yang[a]; Sung-Uk Choi[a]
[a] School of Civil and Environmental Engineering, Yonsei University, Seoul, South Korea

Online publication date: 08 September 2010

To cite this Article Yang, Wonjun and Choi, Sung-Uk(2010) 'A two-layer approach for depth-limited open-channel flows with submerged vegetation', Journal of Hydraulic Research, 48: 4, 466 — 475
To link to this Article: DOI: 10.1080/00221686.2010.491649
URL: http://dx.doi.org/10.1080/00221686.2010.491649

Journal of Hydraulic Research Vol. 48, No. 4 (2010), pp. 466–475
doi:10.1080/00221686.2010.491649

Research paper

A two-layer approach for depth-limited open-channel flows with submerged vegetation

WONJUN YANG, Post-Doctoral Research Fellow, *School of Civil and Environmental Engineering, Yonsei University, Seoul 120-749, South Korea.*
Email: pulip@yonsei.ac.kr

SUNG-UK CHOI (IAHR Member), Professor, *School of Civil and Environmental Engineering, Yonsei University, Seoul 120-749, South Korea.*
Email: schoi@yonsei.ac.kr (author for correspondence)

ABSTRACT
A two-layer approach for depth-limited open-channel flow with submerged vegetation is described. A momentum balance is applied to each layer and expressions for the mean velocities are proposed. The velocity is assumed to be uniform in the vegetation layer and logarithmic in the upper layer. The proposed relationship successfully predicts the mean velocity distribution when compared with the measured data. Using the velocity formula, the layer-averaged mean velocities in the upper layer and over the entire layer are derived. An expression for the roughness coefficient increased by vegetation is also presented, performing better for the roughness coefficient than other formulas. Another relationship is proposed for predicting the distribution of suspended sediment in depth-limited flow with submerged vegetation by using an eddy-viscosity profile. The predicted profiles moderately agree with the measured data. Comparisons with simulated data from the Reynolds-averaged Navier–Stokes equations with the k–ε model suggest that these proposals successfully predict suspended sediment transport in a depth-limited flow with submerged vegetation.

Keywords: Eddy viscosity, open-channel flow, sediment transport, two-layer, vegetation

1 Introduction

Vegetation in a watercourse alters the mean and turbulent flow structures. Such changes in the mean flow and turbulent statistics affect channel conveyance and the transport characteristics related to contaminants and sediment. Thus, an understanding of vegetated flows is essential to better manage floods and the ecosystem of the stream.

Nepf and Vivoni (2000) classified flows with vegetation essentially into three types, depending on the depth ratio, defined by H/h_1, where H is the total flow depth and h_1 is the height of the vegetation layer. If $H/h_1 > 5$ to 10, terrestrial canopy flow occurs which is analogous to flow over a rough boundary. If $H/h_1 < 1$, flow through emergent vegetation results, characterized by a reduced mean flow velocity with suppressed turbulence. If the depth ratio has an intermediate value, the flow is classified as depth-limited flow with submerged vegetation. Complications associated with these flow types have been discussed by Nepf and Ghisalberti (2008): a depth-limited flow with submerged vegetation shows an inflection point in the mean velocity profile due to momentum absorption by the vegetation stems, which triggers the Kelvin–Helmholtz instability. The coherent vortices at the interface dominate the streamwise momentum and scalar transfer between the upper and vegetation layers (Gao *et al.* 1989, Ikeda and Kanazawa 1996, Ghisalberti and Nepf 2002), making bottom friction much less important than the interfacial shear due to the stem drag. Incorporating these flow characteristics into practical river engineering works is nearly impossible, and this necessitates the development of depth-averaged models or resistance laws based on bulk flow principles.

Klopstra *et al.* (1997) proposed analytical expressions for the velocity distribution. The velocity profile within the vegetation layer was obtained using the Boussinesq concept, whereas the logarithmic velocity profile for the upper layer was derived using Prandtl's mixing length theory. Darby (1999) examined previously proposed empirical formulas and described a procedure for computing the friction factor increase by vegetation, thereby accounting also for the flexibility and vitality of the

Revision received 19 April 2010/Open for discussion until 28 February 2011.

ISSN 0022-1686 print/ISSN 1814-2079 online
http://www.informaworld.com

vegetation. Stone and Shen (2002) proposed relationships for the mean velocities in the vegetation and upper layers. They used the force balance concept to determine the mean velocity in the vegetation layer and assumed that the mean velocities over the entire depth and in the vegetation layer were similar. To determine a parameter relating the two mean velocities, they used data obtained in laboratory experiments. Huthoff *et al.* (2007) presented a similar two-layer approach by applying the force balance to the vegetation layer, proposing a mean velocity formula that is identical to that proposed below. They expressed the mean velocity in the upper layer using the power law asymptotic of the characteristic velocity in the vegetation layer, obtaining the similarity exponent from the literature data. Huai *et al.* (2009) proposed a three-layer approach by further dividing the vegetation layer into inner and outer layers. However, the contribution of the inner vegetation layer to the overall flow appears to be small.

The purpose of this study was to develop simple relationships based on the two-layer approach for flow and sediment transport in a depth-limited flow with submerged vegetation. The mean velocity relationships, which are uniform and logarithmic in the vegetation and upper layers, respectively, are proposed and tested. Using these, relationships for the mean concentration of suspended sediment are derived. Comparisons with measured data and simulation results obtained by solving the Reynolds-averaged Navier–Stokes (RANS) equations with the k–ε model reveal that the proposed formulas successfully predict the mean concentration of suspended sediment.

2 Two-layer approach

2.1 *Flow model*

For depth-limited open-channel flows with submerged vegetation (Fig. 1), force components such as gravity, bottom shear, stem drag, and interfacial shear affect the overall flow. For uniform flow, the gravity and interfacial shear are balanced by stem drag and bottom shear in the vegetation layer, i.e.

$$\rho g h_1 S + \tau_i = F_D + \tau_b \tag{1}$$

where ρ is the water density, g the gravitational acceleration, S the slope of channel bottom or energy line, τ_i the interfacial shear stress between the vegetation and upper layers, F_D the drag per unit area due to vegetation, and τ_b the bottom shear stress. For rigid stems, the height of the vegetation layer is identical to the vegetation height, while it is the bent height averaged over time and space for flexible stems (Yang and Choi 2009). In Eq. (1), the stem drag F_D per unit area is given by

$$F_D = \frac{1}{2}\rho a C_D h_1 U_1^2 \tag{2}$$

where C_D is the bulk drag coefficient averaged over the vegetation layer, a the vegetation density, and U_1 the layer-averaged velocity in the vegetation layer. The drag coefficient is distributed vertically, depending largely on the vegetation density and the Reynolds number. Herein, $C_D = 1.13$ from Dunn (1996) was used, which is valid for both rigid cylinder-type and flexible film-type stems (Yang and Choi 2009). For natural reed with foliage, larger values of C_D were reported, ranging between 1.46 and 3.1 for vegetation densities between 2.05 and 10 (Kouwen *et al.* 1969, Murota *et al.* 1984, Tsujimoto and Kitamura 1990, Tsujimoto *et al.* 1993, Meijer 1998). A similar force balance in the upper layer leads to

$$\rho g(H - h_1)S = \tau_i \tag{3}$$

Note that the interfacial shear stress tends to reduce the mean velocity by balancing the gravity in the upper layer, whereas it accelerates the flow in the vegetation layer. For this type of flow, compared with bottom shear, stem drag is dominant in the vegetation layer (Nepf and Ghisalberti 2008). Thus, if bottom shear is ignored, the velocity averaged over the vegetation layer is obtained from Eq. (1) as

$$U_1 = \sqrt{\frac{2gHS}{aC_D h_1}} \tag{4}$$

which states that the velocity in the vegetation layer depends on slope, flow depth, and vegetation properties. Specifically, U_1 is proportional to the square root of the depth ratio and slope and is inversely proportional to the square root of the vegetation density and the bulk drag coefficient. In fact, Eq. (4) is identical to that of Huthoff *et al.* (2007), but it can be regarded as extended to flexible stems due to the definition of the height of the vegetation layer.

Regarding the mean velocity in the upper layer, previous studies based on laboratory experiments revealed that the velocity profile is logarithmic (Lopez and Garcia 1998, Nepf and Vivoni 2000, Stephan and Gutknecht 2002, Järvelä 2003, Baptist *et al.* 2007, Nepf and Ghisalberti 2008). Thus, the following velocity distribution is assumed in the upper layer

$$\frac{u_2(z)}{u_*} = \frac{1}{\kappa}\cdot\ln\left(\frac{z}{h_1}\right) + \frac{U_1}{u_*} \tag{5}$$

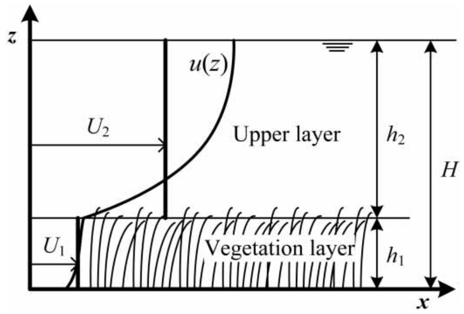

Figure 1 Sketch of depth-limited open-channel flows with submerged vegetation

where $u_2(z)$ is the vertical distribution of mean velocity at the upper layer, u_* the interfacial shear velocity atop of the vegetation layer at $z = h_1$, and κ ($= 0.41$) the von Karman constant. Note in Eq. (5) that $u_2(z = h_1) = U_1$, determining the log-law constant. Similar to open-channel flows with small relative submergence (Dittrich and Koll 1997) and open-channel flows with submerged vegetation (Poggi *et al.* 2004), Yang and Choi (2009) indicated that Eq. (5) should be modified for flows with high vegetation density such as for $a > 5.0$ m^{-1}. Thus, Yang and Choi (2009) proposed

$$\frac{u_2(z)}{U_1} = \frac{u_*}{U_1} \cdot \frac{C_u}{\kappa} \cdot \ln\left(\frac{z}{h_1}\right) + 1 \tag{6}$$

with $C_u = 1$ for $a \leq 5.0$ m^{-1} and $C_u = 2$ for $a > 5.0$ m^{-1}. The density limit of $a = 5$ m^{-1} proposed herein can vary significantly depending on stem flexibility. For the interfacial shear velocity in Eq. (5), Nepf and Ghisalberti (2008) and Yang and Choi (2009) proposed with h_2 ($= H - h_1$) = height of upper layer

$$u_* = \sqrt{g h_2 S} \tag{7}$$

2.2 *Layer-averaged velocity*

Although the logarithmic function approximates the velocity profile in the upper layer well, information on the layer-averaged velocities over the upper layer or whole depth is necessary. Integrating Eq. (6) leads to the layer-averaged velocity in the upper layer

$$U_2 = \frac{C_u \cdot u_*}{\kappa} \cdot \left[\frac{H}{h_2} \cdot \ln\left(\frac{H}{h_1}\right) - 1\right] + U_1 \tag{8}$$

suggesting a dependency on U_1, u_*, and the depth ratio. Equation (8) also reveals that the velocity difference between the two layers increases monotonically, i.e. it is large for $H/h_1 < 10$ and becomes relatively uniform for $H/h_1 > 30.0$. Using the continuity equation, the velocity averaged over the whole depth can be derived as

$$U = U_1 + \frac{C_u \cdot u_*}{\kappa}\left[\ln\left(\frac{H}{h_1}\right) - \frac{h_2}{H}\right] \tag{9}$$

indicating that U exceeds U_1 by the second term on the right-hand side of Eq. (9).

2.3 *Roughness coefficient due to vegetation*

As stated, vegetation in a watercourse increases flow resistance by adding a drag force. The complexity associated with vegetative resistance lies in stem flexibility, the deformation of fronds, seasonal vegetation variability, or non-uniformity of vegetation density (Armanini *et al.* 2005). Thus, instead of taking all of these factors into account, a roughness coefficient is preferred that is increased by vegetation presence. Empirical and quasi-analytical formulas have been proposed. Darby (1999) and Hoffmann and Meer (2002) suggested quasi-analytical formulas, whereas Kouwen and Unny (1973), Thompson and Robertson (1976), Ree and Crow (1977), and Temple (1982) presented empirical formulas for the roughness coefficient due to vegetation. Herein, the following relationship for the vegetative roughness coefficient is proposed by applying Eq. (9) to Manning's formula

$$n_v = \left[\sqrt{\frac{2 \cdot g \cdot H}{a \cdot C_D \cdot h_1}} + \frac{C_u \sqrt{g \cdot h_2}}{\kappa} \cdot \ln\left(\frac{H}{h_1}\right) - \frac{h_2}{H} \cdot \frac{\sqrt{g \cdot h_2}}{\kappa}\right]^{-1} \cdot H^{2/3} \tag{10}$$

which is a function of flow depth and vegetation properties. For flexible stems, the estimation of the bent height is critical when applying Eq. (10) because it is generally a function of the flexural stem rigidity and flow intensity (Kouwen and Li 1980, Tsujimoto *et al.* 1996, Velasco *et al.* 2005, Wilson 2007). Various methods are available for predicting this bent height. Using the experimental data, Wilson (2007) proposed a simple relationship for the bent height as a function of flow velocity. Kouwen and Li (1980) gave an empirical relationship in terms of flexural rigidity and flow intensity. A similar relationship was suggested by Tsujimoto *et al.* (1996) by applying the cantilever beam theory to estimate the bent height. The drag coefficient affects both U and n_v. For a fixed discharge, the roughness coefficient of Eq. (10) increases with the drag coefficient, decreasing average velocities in both vegetation and upper layers and velocity averaged over the entire depth. However, due to the change of the depth ratio, average velocity and roughness are not so sensitive to C_D as implied by Eqs (4) and (10).

2.4 *Suspended sediment transport model*

Under steady equilibrium flow condition of suspended sediment, the vertical distribution of suspended sediment is obtained by integrating the equation

$$v_s c + D_d \frac{\partial c}{\partial z} = 0 \tag{11}$$

where c is the mean concentration and v_s and D_d the particle fall velocity and eddy diffusivity of suspended sediment, respectively. To obtain the suspended sediment concentration, the eddy diffusivity in Eq. (11) is determined first. Relying on the eddy-viscosity concept, the eddy viscosity ν_t is expressed as

$$\nu_t = \frac{-\overline{uw}}{\partial u / \partial z} \tag{12}$$

where $-\overline{uw}$ is the Reynolds shear stress. Nepf and Ghisalberti (2008) and Yang and Choi (2009) reported that a linear function, increasing from zero at the water surface to the maximum at h_1, successfully approximates the Reynolds shear stress of the upper layer. This results in a parabolic profile of the eddy viscosity in the overlying layer. The eddy viscosity, zero at the free surface, increases parabolically to the maximum at a height slightly larger than h_1 and decreases in a similar manner. However, in the vegetation layer, the use of Eq. (12) fails to give the eddy viscosity because of the uniform velocity profile in the vegetation layer. Herein, a "linear bridge", connecting the value at h_1 to zero at the bottom, is assumed for the eddy viscosity, resulting in

$$\nu_t = z \cdot \frac{u_* \kappa}{C_u} \cdot \left(\frac{H - z}{h_2} \right) \quad \text{(upper layer)} \tag{13a}$$

$$\nu_t = z \cdot \frac{u_* \kappa}{C_u} \quad \text{(vegetation layer)} \tag{13b}$$

If the turbulent Schmidt number is assumed to be unity, i.e. eddy diffusivity is identical as eddy viscosity, then Eq. (11) can be integrated using Eqs (13a) and (13b), resulting in the distribution of suspended sediment in

$$\frac{c}{c_b} = \left(\frac{z_b}{z} \right)^Z \left(\frac{H - z}{z} \cdot \frac{h_1}{h_2} \right)^{Z'} \quad \text{(upper layer)} \tag{14a}$$

$$\frac{c}{c_b} = \left(\frac{z_b}{z} \right)^Z \quad \text{(vegetation layer)} \tag{14b}$$

where subscript b denotes "near-bed". Thus, $c(z = z_b) = c_b$, where z_b is normally taken as the height equal to 5% of flow depth. In Eq. (14), $Z = v_s/\kappa u_* =$ Rouse parameter and $Z' = Zh_2/H$.

3 Applications and results

3.1 *Flow model*

Figure 2 shows the vertical distribution of mean velocity in the vegetation layer. Measured data from Meijer (1998), Wilson *et al.* (2003), and Ghisalberti and Nepf (2004) are provided for comparisons. Note that the measured data collapse moderately: the mean velocity decreases slightly up to $z/h_1 = 0.7$ from the interface and becomes uniform thereafter. The constant mean velocity below $z/h_1 = 0.7$ seems to be related to the penetration depth zone where no vertical transport of momentum is present for the zero Reynolds shear stress. The figure also suggests that the uniform velocity assumption within the vegetation layer is acceptable and Eq. (4) predicts the mean velocity quite accurately.

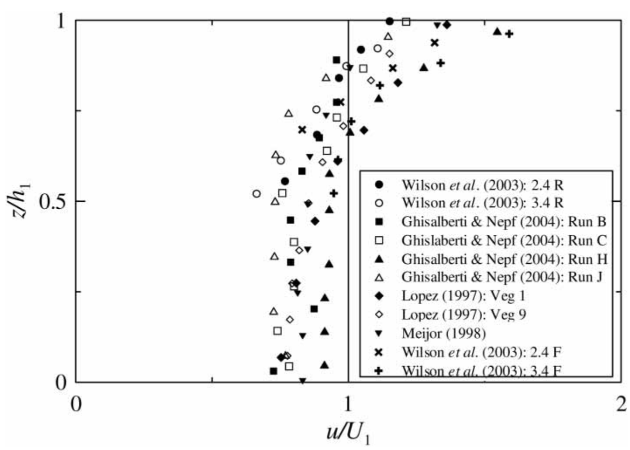

Figure 2 Vertical distribution of mean velocity in vegetation layer

Figure 3 shows the vertical distribution of mean velocity in the upper layer for $a < 5.0$ m^{-1} and $a > 5.0$ m^{-1}. It can be seen that the velocity profile predicted by Eq. (6) is in moderate agreement with the measured data. In comparison with the data of Ghisalberti and Nepf (2004), the predicted mean velocity deviates significantly from the observations particularly near the free surface. This is due to the velocity dip caused by the small width-to-depth ratio of 0.81 used in their experiments.

The mean velocities given by Eqs (4) and (6) are now applied to Yang and Choi's (2009) data. Figure 4 shows the velocity profiles proposed herein and data reported by Yang and Choi (2009) for laboratory experiments under a depth-limited open-channel flow with submerged vegetation. They used both flexible (label F) and rigid (label R) stems. The depth ratio H/h_1 ranged from 2.14 to 3.55 with $a = 2.78$ m^{-1}. The Froude number ranged between 0.15 and 0.41, and the Reynolds number from 15,700

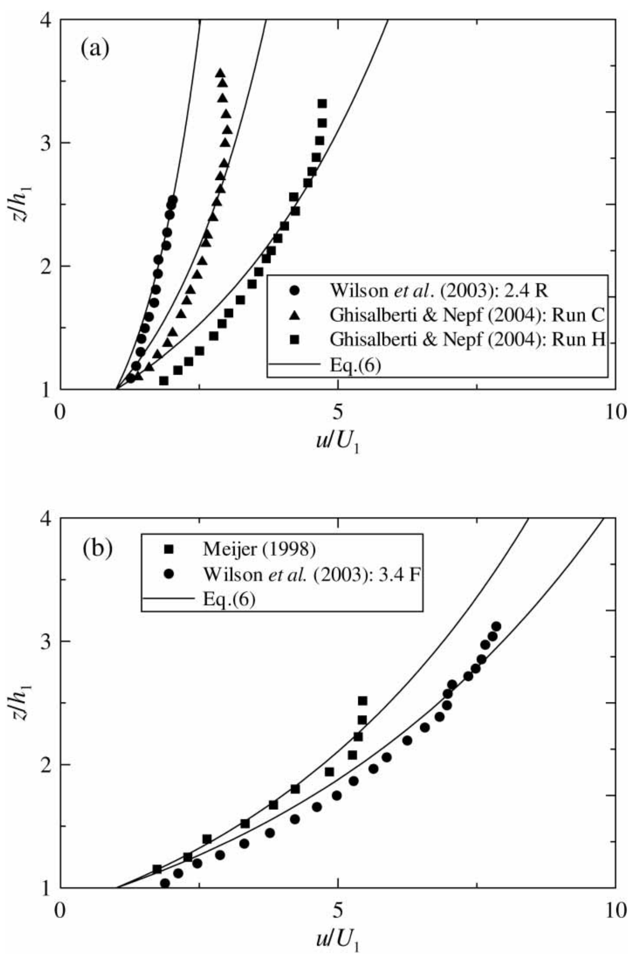

Figure 3 Vertical distribution of mean velocity in upper layer for (a) $a < 5.0$ m^{-1}, (b) $a > 5.0$ m^{-1}

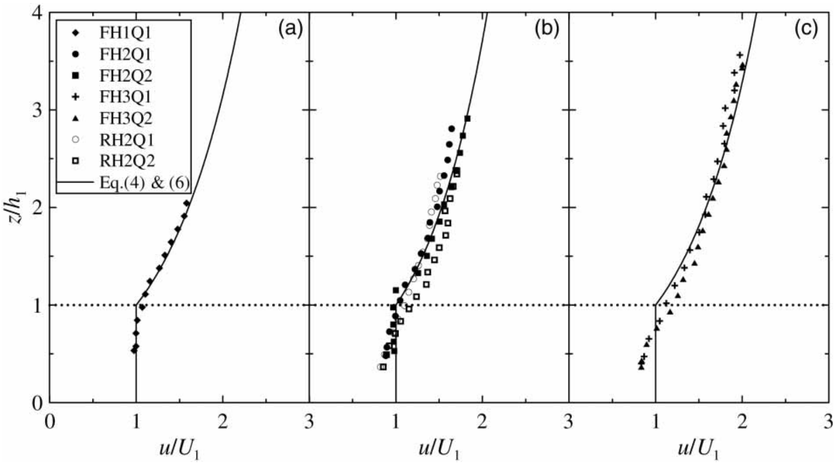

Figure 4 Application of the two-layer model to Yang and Choi's (2009) experiments for $H =$ (a) 0.055 m, (b) 0.075 m, (c) 0.11 m

to 26,300. Note that the model predicts the velocity moderately well, regardless of stem flexibility. However, the profiles predicted by the two-layer model do not have an inflection point near the vegetation height, whereas the measured data do.

3.2 *Layer-averaged velocity*

Layer-averaged mean velocity formulas proposed herein by Eqs (4) and (8) are compared with those developed by Stone and Shen (2002) and Huthoff *et al.* (2007). Note that the formula for U_1 from the present study is identical to that proposed by Huthoff *et al.* (2007). The data sets of Ikeda and Kanazawa (1996), Lopez (1997), Meijer and Velzen (1999), Nepf and Vivoni (2000), Wilson *et al.* (2003), Ghisalberti and Nepf (2004), and Yang and Choi (2009) are compared together with the root-mean-square errors in Fig. 5. In general, the prediction errors in the vegetation layer are less than 10%, smaller than those in the upper layer. It can be seen that Eqs (4) and (8) predict the layer-averaged velocities best, whereas the accuracies of the other two formulas are similar.

Figure 6 successfully compares the velocity averaged over the entire layer predicted by Eq. (9) with the data of Baptist *et al.* (2007). A total of 177 data sets are considered with 74 for flexible (Ikeda and Kanazawa 1996, Meijer 1998, Järvelä 2003) and 103 for rigid vegetation (Kouwen *et al.* 1969, Ree and Crow 1977, Murota *et al.* 1984, Tsujimoto and Kitamura 1990, Tsujimoto *et al.* 1993, Garcia *et al.* 2004). Some experiments include vegetation with fronds (Meijer 1998, Järvelä 2003). The depth ratio lies between 1.25 and 8.07, vegetation density ranges between 0.27 m^{-1} and 33.6 m^{-1}, with the vegetation diameter ranging 0.00024–0.008 m. The Reynolds and Froude numbers, whose characteristic length and velocity are flow depth and depth-averaged mean velocity, cover the range from 45,000 to 3,000,000 and from 0.02 to 0.57, respectively. Values of drag coefficients if stated were used, namely 3.0 in Kouwen *et al.* (1969), 2.75 in Murota *et al.* (1984), 1.46 in Tsujimoto and Kitamura (1990), 2.0 in Tsujimoto *et al.* (1993), 1.81 in Meijer (1998), and 1.13 otherwise.

3.3 *Roughness coefficients due to vegetation*

Figure 7 compares predicted with estimated roughness coefficients. Formulas, including those of Thompson and Robertson (1976), Darby (1999), Hoffmann and Meer (2002), and Eq. (10) are considered. The data were taken from Ikeda and Kanazawa (1996), Lopez (1997), Nepf and Vivoni (2000), Wilson *et al.* (2003), Ghisalberti and Nepf (2004), Garcia *et al.* (2004), Ghisalberti and Nepf (2006), and Yang and Choi (2009). Note that Eq. (10) and Darby's (1999) formula slightly over-predict the roughness coefficient. The accuracy of these two relationships appears to be similar. However, for $n_v > 0.06$, Darby's formula results in a slight overestimation. In contrast, Hoffmann and Meer's (2002) formula significantly overestimates n_v, and Thompson and Robertson (1976) significantly under- and over-predict the data. Although none of these formulas account for stem flexibility, Eq. (10) allows us to consider stem flexibility if the height of the vegetation layer and the drag coefficient stems are given for flexible vegetation.

Figure 8 compares measured and estimated roughness coefficients for the data set of Baptist *et al.* (2007). For $n_v \leq 0.07$, Eq. (10) predicts the roughness coefficient appropriately. However, for $n_v > 0.07$, the equation appears to overestimate the roughness coefficient. The data in this specific range were taken from Ree and Crow (1977), Kouwen (1988), and Meijer (1998) for flexible stems at high vegetation densities and low depth ratios. Kouwen (1988) attributed the reduced roughness to a shielding effect: in a flow with a high density of flexible vegetation, the stem directly behind other stems are shielded from the flow force with a densely planted group of stems providing a larger shielding effect when compared to a single or coarsely planted stems. This effect tends to reduce resistance for flow with flexible vegetation at high densities.

3.4 *Suspended sediment transport model*

The relationships for the eddy viscosity given by Eq. (13) are tested herein. Figure 9 shows its vertical distribution for *a*

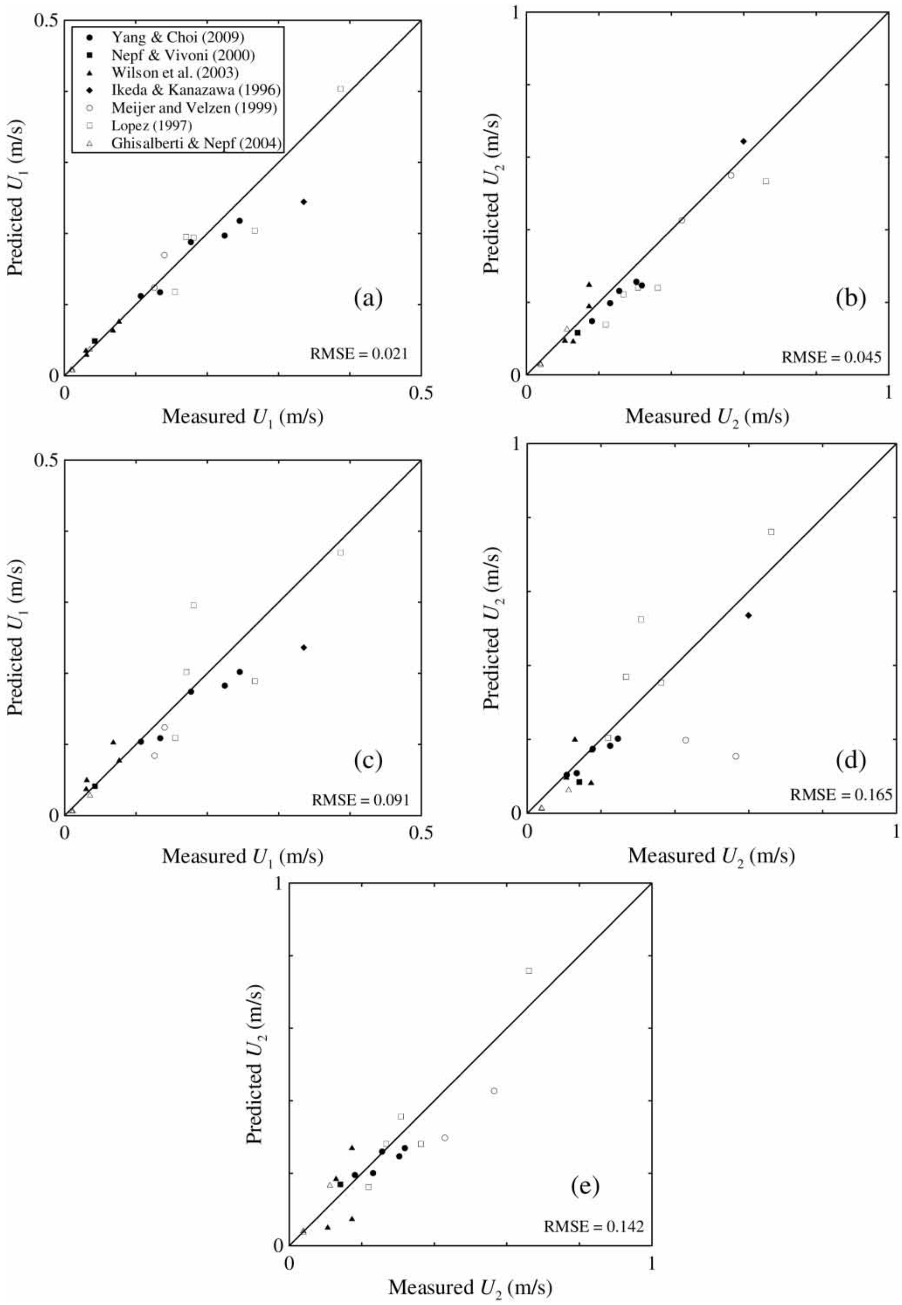

Figure 5 Comparison between predicted and measured layer-averaged velocities in (a) vegetation layer and Eq. (4), (b) upper layer and Eq. (8), (c) vegetation layer and Stone and Shen's formula, (d) upper layer and Stone and Shen's formula, (e) upper layer and Huthoff *et al.*'s formula

$< 5.0\ \text{m}^{-1}$ and $a > 5.0\ \text{m}^{-1}$, respectively, based on the laboratory data of Lopez and Garcia (1998) and Yang and Choi (2009), and numerical simulations using the Reynolds stress model (Choi and Kang 2004). In general, the eddy viscosity in the upper layer is larger than that in the vegetation layer, which is consistent with findings from field observations reported by Ackerman (2002).

For $a < 5.0\ \text{m}^{-1}$, both measured data and predicted profile show a maximum above h_1 in the upper layer but Eq. (13a) appears to slightly over-predict the maximum eddy viscosity. Similarly, in the vegetation layer, Eq. (13b) slight over-predicts. However, a general trend observed in the measured data conforms that in the predicted profile. For $a > 5.0\ \text{m}^{-1}$, the eddy viscosity by the Reynolds stress model has a maximum close to the free surface compared with Eq. (13a). Measured data reported by Lopez and Garcia (1998), only available for $z/h_1 < 2.0$, gives a moderate match to the profile obtained from Eqs. (13) but the match is favourable to the profile simulated by the Reynolds stress model.

The model for suspended sediment transport was applied to the experimental data reported by Yuuki and Okabe (2002), who conducted flume experiments with submerged vegetation. Their flume was 12 m long and 0.4 m wide. Their experiments employed a fixed flow depth of $H = 0.06$ m considering Case

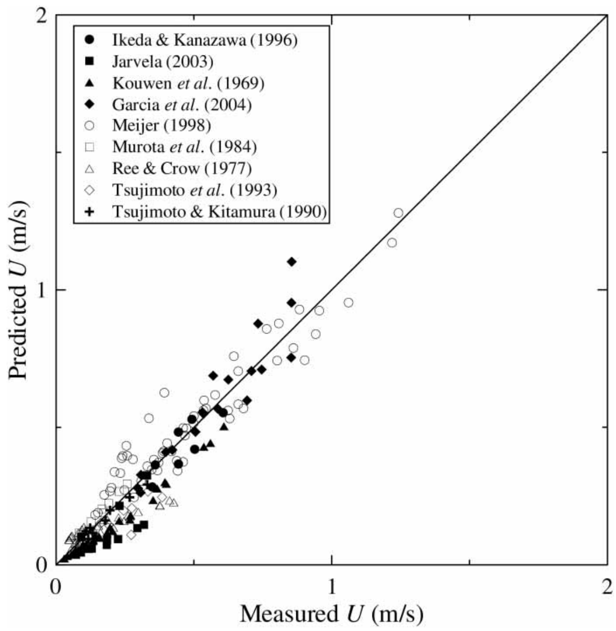

Figure 6 Comparison between predicted and measured average velocities over whole depth

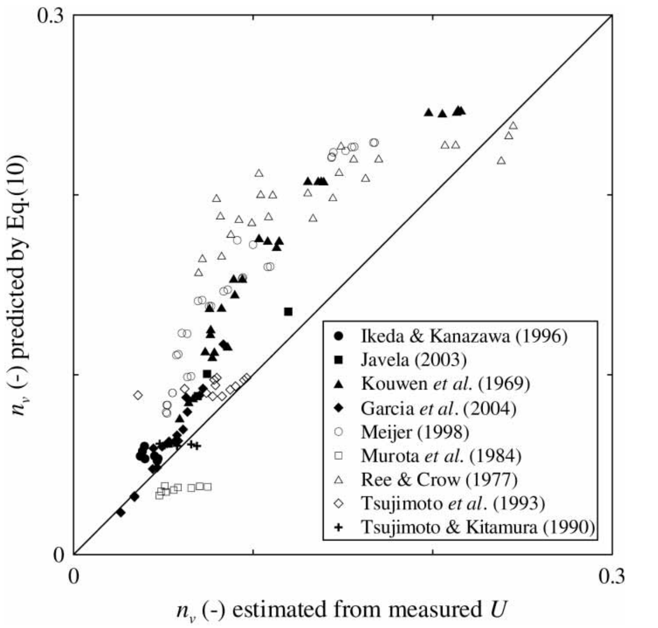

Figure 8 Comparison between measured and predicted Manning's roughness coefficients

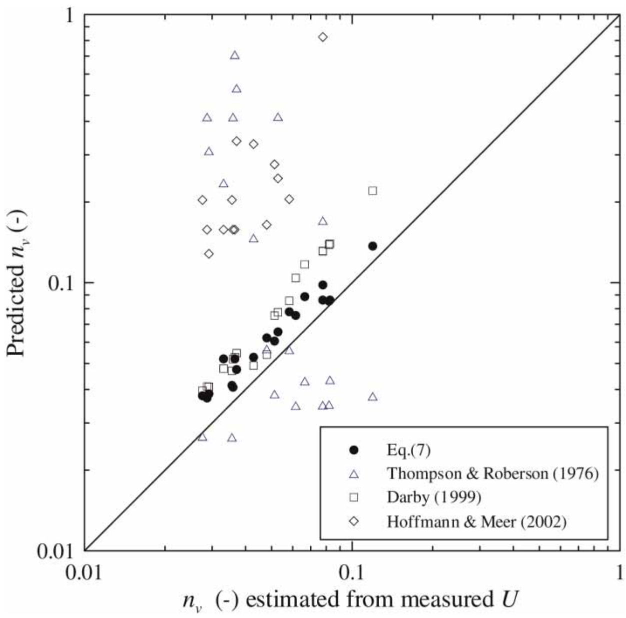

Figure 7 Comparison of various formulas for Manning's roughness coefficient

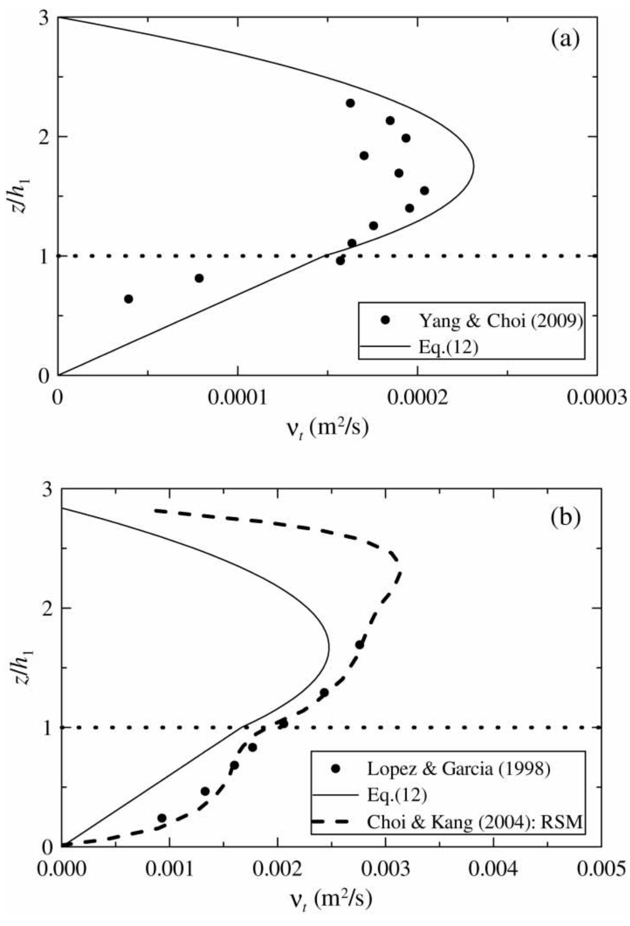

Figure 9 Vertical distribution of eddy viscosity for (a) $a < 5.0\ \mathrm{m}^{-1}$, (b) $a > 5.0\ \mathrm{m}^{-1}$

1: $Q = 0.00545\ \mathrm{m}^3/\mathrm{s}$, $S = 0.001$; Case 2: $Q = 0.00675\ \mathrm{m}^3/\mathrm{s}$, $S = 0.0015$; and Case 3: $Q = 0.00765\ \mathrm{m}^3/\mathrm{s}$, $S = 0.002$. The corresponding Rouse parameters are $Z = 0.26$, 0.21, and 0.18, respectively. They obtained the equilibrium suspension of sediment particles by increasing the concentration before deposition occurred and measured the sediment concentration by the direct suction. They used mimic vegetation consisting of five 0.5 mm thick bronze wires bundled with a 5 mm long aluminium pipe and polyvinyl sediment particles of size $D_s = 0.1$ mm and specific gravity of 1.42.

Figure 10 shows the vertical distribution of suspended sediment concentration. Profiles predicted by Eq. (14) are given along with the measured data. Note that the predicted profiles moderately agree with the measured data. Specifically, the mean concentration of the upper layer predicted by the present model is higher than that from the measured data. In contrast, the mean concentration by Eq. (14b) appears to be under-predicted in the vegetation layer. This may be attributed to the assumption of unity turbulent Schmidt number because the rate of scalar diffusion differs significantly from that of momentum in vegetated flows than in plain open-channel flows (Kang *et al.* 2009).

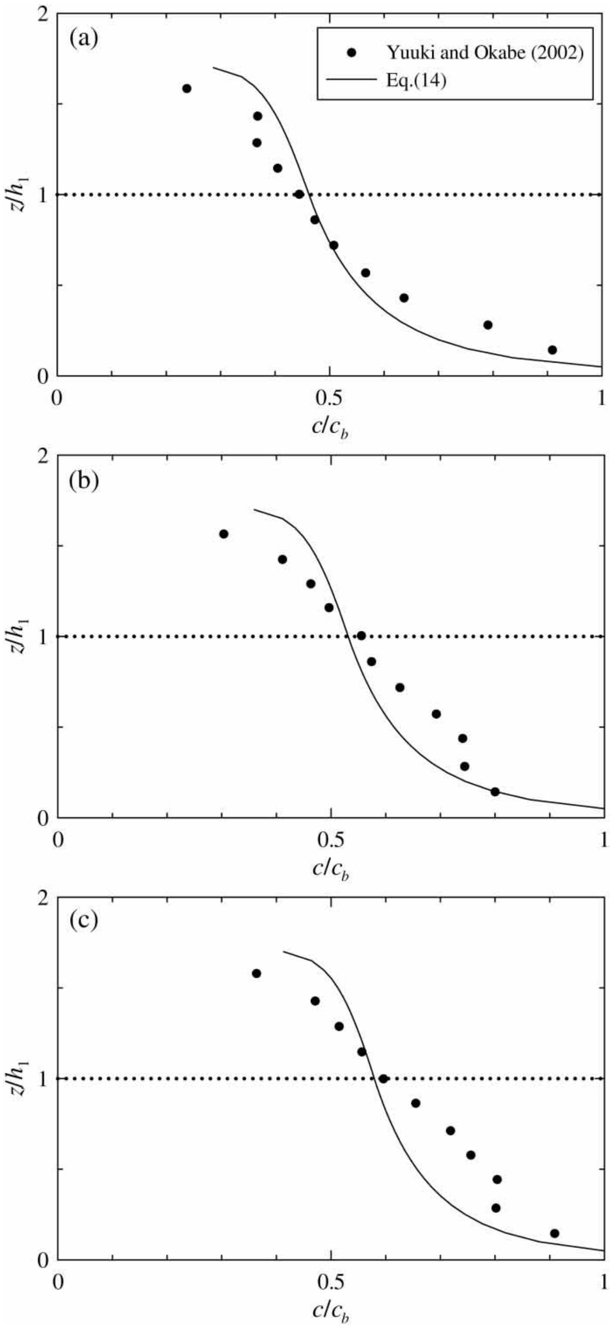

Figure 10 Vertical distribution of suspended sediment concentration for (a) Case 1 ($Z = 0.26$), (b) Case 2 ($Z = 0.21$), (c) Case 3 ($Z = 0.18$)

Finally, the concentration profiles of suspended sediment predicted by the two-layer approach are compared with those obtained by solving the RANS equations using the k–ε model and the numerical model of Kang and Choi (2005). A submerged vegetation flow was assumed to have the following flow and vegetation characteristics: $H = 0.3$ m, $S = 0.0005$, $h_1 = 0.1$ m, and $a = 1.0$ m^{-1}. Figure 11 shows the distribution of suspended sediment concentration for various Rouse parameters and depth ratios, respectively. Both profiles from Eq. (14) and numerical simulations are given for comparison. The profile by the proposed relationships in Fig. 11(a) shows that the sediment particles become more uniformly distributed as the Rouse parameter decreases, or the particle fall velocity decreases as the interfacial shear velocity increases. This trend is observed in profiles simulated by the k–ε model. A similar conclusion was given by Lopez and Garcia (1998). However, compared with the simulated profiles, Eq. (14) under- and over-estimates the suspended sediment concentration in the upper and vegetation layers, respectively, as also was observed for Yuuki and Okabe's (2002) data. The effect of depth ratio is shown in Fig. 11(b). As the depth ratio increases, the suspended sediment concentration profile becomes more uniform over the entire column. This is reasonable because the increased depth ratio involves a decreased impact of submerged vegetation on suspended sediment distribution.

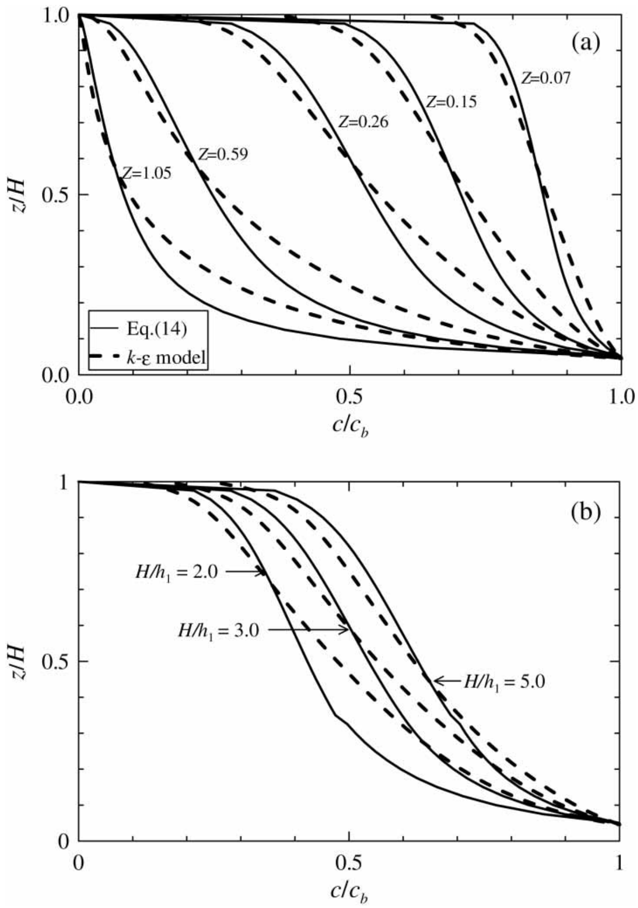

Figure 11 Comparison of suspended sediment concentration. Effect of (a) Z for $H/h_1 = 3.0$, (b) depth ratio for $Z = 0.26$

4 Conclusions

A two-layer approach is proposed for depth-limited open-channel flows with submerged vegetation. The flow model assumes a uniform and a logarithmic velocity distribution in the vegetation and upper layers, respectively. The momentum balance was applied to both layers to obtain the velocity model. Good agreement was obtained if the flow model is applied to laboratory experiments. Relationships for the velocity averaged over the upper layer and over the whole layer are also presented. The proposed relationships predict the velocity best, suggesting that the flow model is capable of predicting correctly the conveyance of a vegetated channel.

A model for suspended sediment transport in a flow with submerged vegetation was then presented. In the upper layer, a parabolic distribution of eddy viscosity is proposed with the maximum slightly above the vegetation layer. A linear distribution of eddy viscosity, decreasing to zero at the bottom, was assumed in the vegetation layer. Comparisons with measured data and a simulated profile using the Reynolds stress model support the validity of this profile. Expressions for the concentration of suspended sediment were then derived. Comparisons with measured data reveal that the model slightly over- and under-predicts sediment concentration above and below the height of the vegetation layer, respectively. Finally, the suspended sediment concentration predicted by the proposed model was compared with simulation results from the RANS equations. The model predicts the distribution of suspended sediment moderately well. The model also reproduces the impact of the Rouse parameter and the depth ratio properly. For practical purposes, further studies should focus on the drag coefficient and the bent height of natural vegetation.

Acknowledgement

This work was supported by a grant (Code # '06 CTIP B-01) from the Construction Technology Innovation Program (CTIP) funded by the Ministry of Land, Transport, and Maritime Affairs of the Korean Government.

Notations

a	planting density of vegetation
C_D	bulk drag coefficient averaged over h_1
C_u	coefficient for $u_2(z)$ in Eq. (6)
c	mean suspended sediment concentration
c_b	near-bed concentration of suspended sediment
D_d	eddy diffusivity of suspended sediment
D_s	mean diameter of suspended sediment particles
F_D	drag force per unit area due to vegetation
g	gravitational acceleration
H	total flow depth
h_1	height of vegetation layer
h_2	height of upper layer
n_v	Manning's roughness coefficient
S	bottom slope
U	averaged velocity over entire layer
U_1	layer-averaged velocity at vegetation layer
U_2	layer-averaged velocity at upper layer
u_*	interfacial shear velocity atop of vegetation layer
$u_2(z)$	mean velocity at upper layer
$-\overline{uw}$	Reynolds shear stress
Z	modified Rouse parameter for vegetation layer
Z'	modified Rouse parameter for upper layer
z	distance from bottom
z_b	reference height for c_b
κ	von Karman constant
ν_s	terminal fall velocity
ν_t	eddy viscosity
ρ	water density
τ_b	bottom shear stress
τ_i	interfacial shear stress between vegetation and upper layers

References

Ackerman, J.D. (2002). Diffusivity in a marine macrophyte canopy: Implications for submarine pollination and dispersal. *American J. Botany* 89(7), 1119–1127.

Armanini, A., Righetti, M., Grisenti, P. (2005). Direct measurement of vegetation resistance in prototype scale. *J. Hydraulic Res*. 43(5), 481–487.

Baptist, M.J., Babovic, V., Rodriguez Uthurburu, J., Uittenbogaard, R.E., Mynett, A., Verwey, A. (2007). On inducing equations for vegetation resistance. *J. Hydraulic Res*. 45(4), 435–450.

Choi, S.U., Kang, H. (2004). Reynolds stress modelling of vegetated open-channel flows. *J. Hydraulic Res*. 42(1), 3–11.

Darby, S.E. (1999). Effect of riparian vegetation on flow resistance and flood potential. *J. Hydraulic Engng*. 125(5), 443–454.

Dittrich, A., Koll, K. (1997). Velocity field and resistance of flow over rough surfaces with large and small relative submergence. *Int. J. Sediment Res*. 12(3), 21–33.

Dunn, C.J. (1996). Experimental determination of drag coefficients in open-channel with simulated vegetation. *M. Thesis*. University of Illinois, Urbana-Champaign, Urbana, IL.

Gao, W., Shaw, R.H., Paw, K.T. (1989). Observation of organized structure in turbulent flow within and above a forest canopy. *Boundary-Layer Meteorol*. 47, 349–377.

Garcia, M.H., Lopez, F., Dunn, C., Alonso, C. (2004). Flow, turbulence, and resistance in a flume with simulated vegetation. *Riparian Vegetation and Fluvial Geomorphology, Water Science and Application* 9, 11–27, S.J. Bennet, A. Simon, eds. American Geophysical Union, Washington, DC.

Ghisalberti, M., Nepf, H.M. (2002). Mixing layers and coherent structures in vegetated aquatic flow. *J. Geophy. Res*. 107(C2), 1–11.

Ghisalberti, M., Nepf, H.M. (2004). The limited growth of vegetated shear layers. *Water Resour. Res*. 40(7), W07052.

Ghisalberti, M., Nepf, H.M. (2006). The structure of the shear layer in flows over rigid and flexible canopies. *Env. Fluid Mech*. 6, 277–301.

Hoffmann, M.R., Meer, F.M. (2002). A simple space-time averaged porous media model for flow in densely vegetated channels. *Computational Methods and Water Res*. 2(47), 1661–1668.

Huai, W.X., Zeng, Y.H., Xu, Z.G., Yang, Z.H. (2009). Three-layer model for vertical distribution in open channel flow with submerged rigid vegetation. *Adv. Water Resour*. 32(4), 487–492.

Huthoff, F., Augustijn, D.C.M., Hulscher, S.J.M.H. (2007). Analytical solution of the depth-averaged flow velocity in case of submerged rigid cylindrical vegetation. *Water Resour. Res*. 43(6), W06413.

Ikeda, S., Kanazawa, M. (1996). Three-dimensional organized vortices above flexible water plants. *J. Hydraulic Engng*. 122(11), 634–640.

Järvelä, J. (2003). Influence of vegetation on flow structure in floodplains and wetlands. Proc. 3rd *River, Coastal and Estuarine Morphodynamics*, Madrid, 845–856.

Kang, H., Choi, S.U. (2005). Anisotropy of turbulence in vegetated open-channel flows. *J. KWRA* 38(10), 871–883 [in Korean].

Kang, H., Choi, S.U., Choi, B. (2009). Solute transport in open-channel flows with submerged vegetation. Proc. 33rd *IAHR Congress*, Vancouver, Canada, CD-ROM.

Klopstra, D., Barneveld, H.J., Noortwijk, J.M., Velzen, E.H. (1997). Analytical model for hydraulic roughness of submerged vegetation. Proc. 27th *IAHR Congress*, San Francisco, Theme A 2, 775–780.

Kouwen, N. (1988). Field estimation of the biomechanical properties of grass. *J. Hydraulic Res*. 26(5), 559–569.

Kouwen, N., Li, R. (1980). Biomechanics of vegetative channel linings. *J. Hydraulics Div.* ASCE 106(HY6), 1085–1103.

Kouwen, N., Unny, T.E. (1973). Flexible roughness in open channels. *J. Hydraulics Div.* ASCE 99(HY5), 713–728.

Kouwen, N., Unny, T.E., Hill, H.M. (1969). Flow retardance in vegetated channel. *J. Irr. Drainage Div.* ASCE 95(IR2), 329–340.

Lopez, F. (1997). Open-channel flow with roughness elements of different spanwise aspect ratios: Turbulent structure and numerical modeling. *PhD Thesis*. University of Illinois at Urbana-Champaign, Urbana, IL.

Lopez, F., Garcia, M.H. (1998). Open-channel flow through simulated vegetation: Suspended sediment transport modeling. *Water Resour. Res*. 34(9), 2341–2352.

Meijer, D.G. (1998). Model test submerged vegetation, physical model investigation. *Report of HKV Consultants*, Rijkswaterstaat/RIZA, Den Haag [in Dutch].

Meijer, D.G., Velzen, E.H. (1999). Prototype-scale flume experiments on hydraulic roughness of submerged vegetation. Proc. 28th *IAHR Congress*, Graz, Austria, CD-ROM.

Murota, A., Fukuhara, T., Sato, M. (1984). Turbulence structure in vegetated open channel flows. *Hydroscience and Hydraulic Engng*. 2(1), 47–61.

Nepf, H., Ghisalberti, M. (2008). Flow and transport in channels with submerged vegetation. *Acta Geophysica*. 56(3), 753–777.

Nepf, H.M., Vivoni, E.R. (2000). Turbulence structures in depth-limited, vegetated flow. *J. Geophy. Res*. 105(C12), 28547–28557.

Poggi, D., Porporato, A., Ridolfi, L. (2004). The effect of vegetation density on canopy sub-layer turbulence. *Boundary-Layer Meteorol*. 111(3), 565–587.

Ree, W.O., Crow, F.R. (1977). Friction factors for vegetated waterways of small slope. *Technical Report Publication* S-151. U.S. Department of Agriculture, Agricultural Research Service, Washington, DC.

Stephan, U., Gutknecht, D. (2002). Hydraulic resistance of submerged flexible vegetation. *J. Hydrol*. 269(1), 27–43.

Stone, B.M., Shen, H.T. (2002). Hydraulic resistance of flow in channels with cylindrical roughness. *J. Hydraulic Engng*. 128(5), 500–506.

Temple, D.M. (1982). Flow retardance of submerged grass channel linings. *Trans. ASAE* 25(5), 1300–1303.

Thompson, G.T., Robertson, J.A. (1976). A theory of flow resistance for vegetated channels. *Trans. ASAE* 19(2), 288–293.

Tsujimoto, T., Kitamura, T. (1990). Velocity profile of flow in vegetated bed channels. *KHL Progressive Report* 1, Kanazawa University, Kanazawa, Japan.

Tsujimoto, T., Kitamura, T., Fujii, Y., Nakagawa, H. (1996). Hydraulic resistance of flow with flexible vegetation in open channel. *J. Hydroscience and Hydraulic Engng*. 14(1), 47–56.

Tsujimoto, T., Okada, T., Kontani, K. (1993). Turbulent structure of open channel flow over flexible vegetation. *KHL Progressive Report* 4. Kanazawa University, Kanazawa, Japan.

Velasco, D., Bateman, A., DeMedian, V. (2005). A new integrated, hydro-mechanical model applied to flexible vegetation in riverbeds. *River, Coastal and Estuarine Morphodynamics* 1, 217–227. G. Parker, M.H. Garcia, eds., University of Urbana-Champaign, Urbana IL.

Wilson, C.A.M.E. (2007). Flow resistance models for flexible submerged vegetation. *J. Hydrol*. 342(3), 213–222.

Wilson, C.A.M.E., Stoesser, T., Bates, P.D., Pinzen, A.B. (2003). Open-channel flow through different forms of submerged flexible vegetation. *J. Hydraulic Engng*. 129(11), 847–853.

Yang, W., Choi, S.U. (2009). Impact of stem flexibility on mean flow and turbulence structure in open-channel flows with submerged vegetation. *J. Hydraulic Res*. 47(4), 445–454.

Yuuki, T., Okabe, T. (2002). Hydrodynamic mechanics of suspended load on riverbeds vegetated by woody plants. *J. JWRA* 46, 701–706 [in Japanese].